01ICES-74

Investigation of Transient Temperature Oscillations of a Propylene Loop Heat Pipe

José I. Rodriguez and Arthur Na-Nakornpanom
Jet Propulsion Laboratory, California Institute of Technology

ABSTRACT

A technology demonstration propylene Loop Heat Pipe (LHP) has been tested extensively in support of the implementation of this two-phase thermal control technology on NASA's Earth Observing System (EOS) Tropospheric Emission Spectrometer (TES) instrument. This cryogenic instrument is being developed at the Jet Propulsion Laboratory (JPL) for NASA. This paper reports on the transient characterization testing results showing low frequency temperature oscillations. Steady state performance and model correlation results can be found elsewhere. Results for transient startup and shutdown are also reported elsewhere.

In space applications, when LHPs are used for thermal control, the power dissipation components are typically of large mass and may operate over a wide range of power dissipations; there is a concern that the LHP evaporator may see temperature oscillations at low powers and over some temperature range. In addition, the LHP may not start when power is applied to the component until a significant temperature overshoot from the equilibrium temperature is developed. In most space applications, the temperature oscillation will pose a problem because the maximum allowable flight temperatures (AFTs) may be exceeded and the long-term reliability of equipment is compromised. When equipment temperature stability is important, this becomes a serious issue. Its important to understand the LHP behavior in such a situation in order to mitigate potential problems and design predictable two-phase thermal control systems.

A test program was developed at JPL to characterize the transient behavior of a propylene LHP with a large mass attached to the evaporator and at low powers and low sink temperatures. The LHP was tested in a horizontal orientation with heat loads ranging from 15 to 75 watts and condenser temperatures from -30°C to 0°C. In addition, a small heater and temperature sensor were placed on the LHP compensation chamber to provide close loop temperature control and was tested under similar conditions. Transient results show repeatable low frequency temperature oscillations for a range of conditions. When temperature control is applied to the compensation chamber, the evaporator temperature oscillations disappear. Recommendations are made for additional research on this topic.

INTRODUCTION

The use of loop heat pipes in thermal control systems has increased significantly over the past few years. NASA as well as other government agencies including private industry have baselined both ammonia and propylene LHPs for thermal control in space applications.

LHPs are passive heat transport devices that use capillary forces to circulate a two-phase working fluid. They consist of a heat-accepting evaporator, heat-rejecting condenser, fluid reservoir and tubing to connect the components. The fundamental theory of LHP operation and detailed descriptions of applications can be found in various papers [1-15]. They were developed in the former Soviet Union in the early 1980's and have flown successfully in a number of space missions. These include the ALYONA flight experiment launched in 1989, the OBZOR optical instrument launched in 1994, both used propylene LHPs and to date both are still operating in space [3,4].

LHPs were selected for use on the TES instrument to solve two key thermal control problems: (1) while in survival mode the instrument equipment must be thermally decoupled from the nadir heat-rejecting radiators to conserve survival heater power and remain within the allocated budget, and (2) enable the packaging of equipment within the instrument envelope and meet the cable length and routing requirements as well as the structural design constraints. Ground test operations dictates that the thermal control system must operate in both horizontal and vertical orientations. Horizontal orientation refers to a condition with the condenser normal to the gravity vector and the evaporator below. Vertical position refers to the condenser parallel to the

gravity vector and the evaporator at an elevation between the extreme rungs of the condenser. The implementation of LHPs provided the required design space to meet all the thermal, electrical, structural, and mechanical configuration requirements. Propylene was selected over ammonia for the TES LHPs to avoid freezing of ammonia while in the spacecraft survival mode. Propylene has a freezing point of –180°C whereas ammonia is only –78°C. A detailed description of the TES instrument thermal control system is available in Ref. 15.

JPL'S LOOP HEAT PIPE TEST BED

A characterization testing program was initiated at JPL to support the implementation of this thermal control technology on the TES instrument. A fully automated test bed was developed to enable testing of LHPs in an ambient environment at any orientation and with capability to vary the condenser sink temperature, initial evaporator temperature and power to evaporator. In addition, heater power can be applied to compensation chamber or closed-loop temperature control can be used to control its temperature. The test bed is shown in Figs. 1-3. The test LHP is supported on a table, which can be rotated to any orientation, with the LHP fully instrumented. The LHP condenser is attached to a 1/8 inch aluminum radiator plate as shown in Fig. 1. A fluid cooling loop is then attached to the opposite side of this radiator plate to provide cooling. The evaporator saddle and condenser radiator plate are supported from the adjustable table using low conductivity G10 rods. An aluminum heater block, mounted to the evaporator saddle, with two calrod heaters is used for providing heat to the evaporator. Similarly, an aluminum cooling block with a fluid heat exchanger is attached to the opposite side of the evaporator saddle to actively control its temperature. The entire LHP is fully insulated with fiberglass and foam insulation material to minimize parasitic heat leaks.

An electronics rack with power supplies, temperature controller, thermocouple readout unit and a chiller, for fluid loop temperature control, was used for controlling and monitoring the test. A LabView™ program was written to automate the tests, provide real-time data monitoring and trending capability and save heater power and thermocouple data in a file.

LHP TECHNOLOGY DEMONSTRATION UNIT

A copy of an existing LHP design was procured from Dynatherm Corporation Inc. to evaluate this technology. The design is based on a LHP manufactured for NASA GSFC's Geoscience Laser Altimeter System (GLAS). The evaporator consists of an all aluminum saddle/body encasing a sintered nickel wick structure. The compensation chamber is made from stainless steel with flat end caps as shown in Fig. 4.

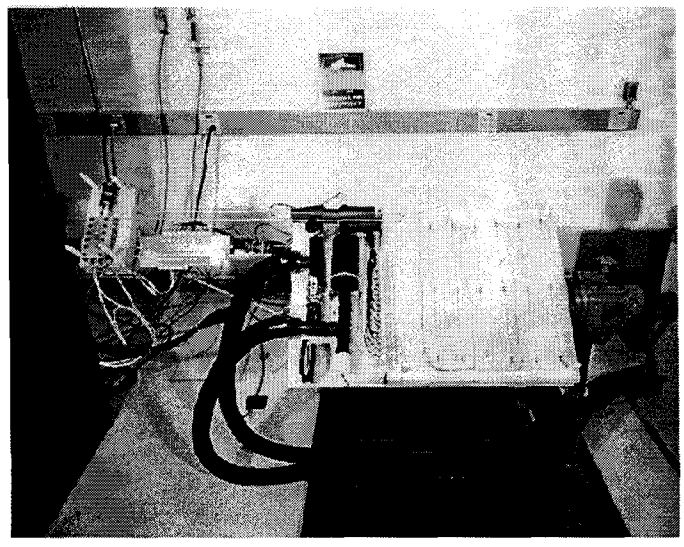

Figure 1. LHP test bed setup: support table

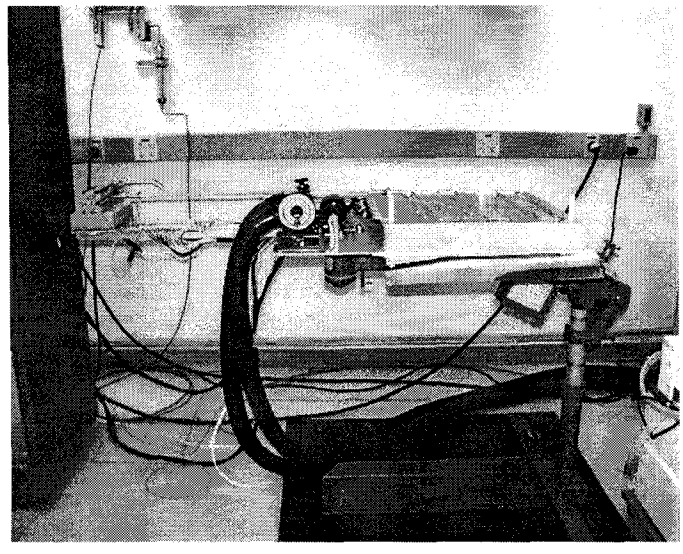

Figure 2. LHP test bed setup: horizontal table position

The transport lines are made from stainless steel tubing and the condenser is made from a single piece of flanged aluminum extrusion shaped into a serpentine configuration. The condenser is mounted on a 1/8 inch aluminum plate with another identical serpentine shape flanged extrusion bent into a mirrored image on the opposite side of the plate. This provides the heat sink using a cooling fluid loop. Fig. 5 shows the condenser mounted to the aluminum plate. The geometric parameters of the LHP are shown in Table 1. A schematic of the LHP with the thermocouple locations is illustrated in Fig. 6.

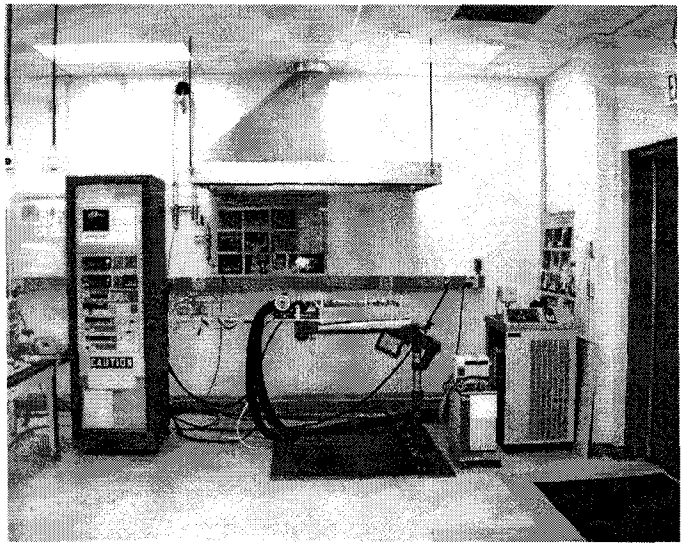

Figure 3. LHP laboratory test bed setup: electronics rack, support table and chiller.

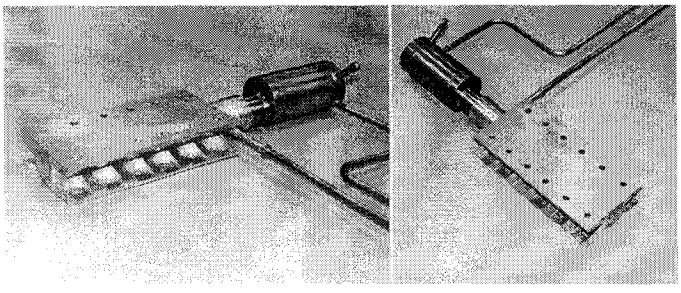

Figure 4. LHP evaporator and compensation chamber

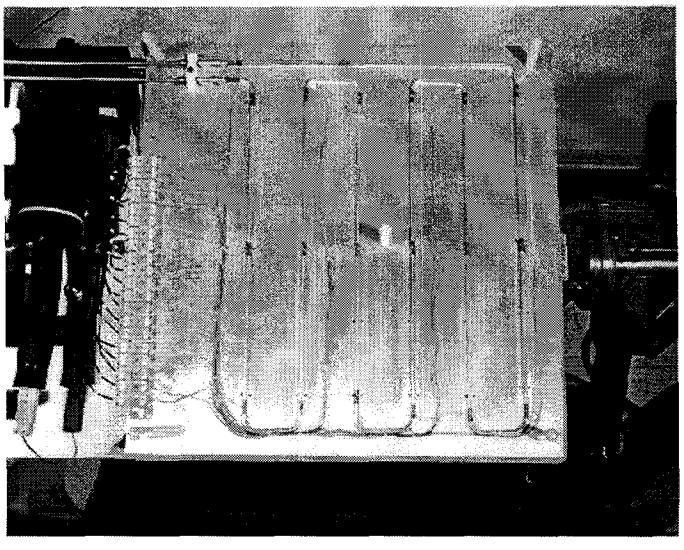

Figure 5. LHP Condenser attached to aluminum plate

A large mass to simulate the TES equipment was attached to the evaporator to study transient phenomena. The large mass consisted of a stack of copper blocks of the same width as the evaporator saddle. All tests were carried out with 21 kg of copper attached to the evaporator. Figs. 7 and 8 show the evaporator with six copper blocks attached. The aluminum heater block is mounted to the top of the copper block stack.

Table 1. Key geometric parameter of test unit

Component	Description
Evaporator	
Material	6061 AL
I.D.	2.421 cm
Length	15.24 cm
Primary wick	
Material	Sintered nickel
Pore size	1.2 μm
Porosity	0.60
Permeability	$4x10^{-14}$ m^2
Compensation chamber	
Material	316L SS
O.D.	4.394 cm
Length	8.025 cm
Volume	115 cm^3
Transport lines	
Material	304L SS
I.D.	0.452 cm
Wall thickness	0.508 mm
Vapor line length	1.00 m
Liquid line length	1.074 m
Condenser	
Material	6063 AL extrusion
I.D.	0.399 cm
Wall thickness	7.62 mm
Length	3.81 m
Propylene	
Charge	80 grams
Purity	99°%
Heating block	
Material	6061 AL
Dimension	7.62 cm by 15.24 cm by 1.91 cm
Mass	0.5 kg
Cooling block	
Material	6061 AL
Dimensions	7.62 cm by 15.24 cm by 1.27 cm
Mass	0.5 kg
Large mass (each block)	
Material	Copper
Dimensions	7.62 cm by 20.32 cm by 2.54 cm
Mass	3.5 kg

The heat capacity of all six copper blocks including the aluminum heater and cooling blocks is 9,080 J/C. This is equivalent to 10.2 kg of aluminum. The equivalent aluminum mass of the evaporator, wick, compensation chamber and liquid core is approximately 0.81 kg. Prior to startup, after power is applied to the large mass, the heater power is used to raise the temperature of the large mass/ evaporator assembly. Assuming parasitic heat leaks are negligible, the power delivered to the evaporator saddle/body can be obtained from a simple energy balance as follows:

$Q_{LHP}=(m/(M+m))Q_{mass}$

Where, **m** is the evaporator and compensation chamber assembly mass, **M** is the mass of the large mass, Q_{mass} is the heater power applied to the large mass.

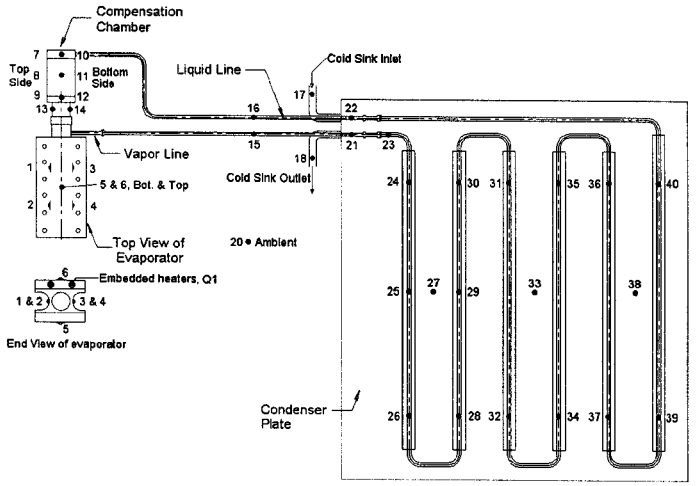

Figure 6. Schematic of LHP with test thermocouples

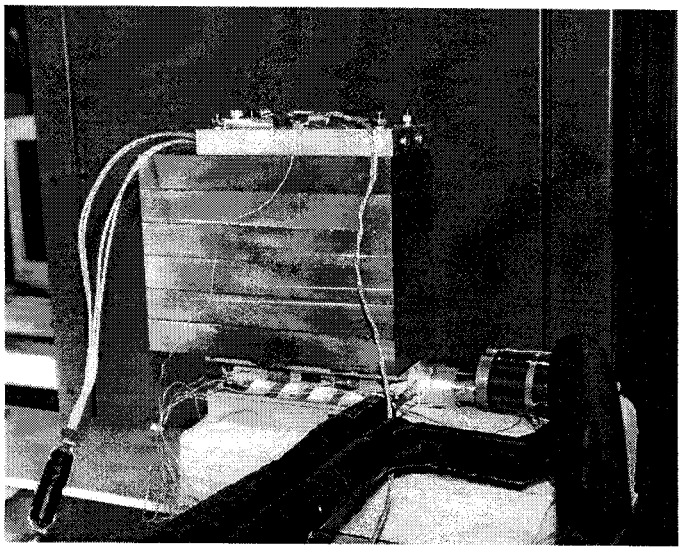

Figure 7. LHP evaporator with large mass: view of heating block on top

Under these conditions a maximum of 7% of the heater power applied to the large mass is delivered to the LHP evaporator saddle to develop the superheat required to initiate boiling. This represents the maximum power available to the evaporator for startup because parasitic heat leaks will only reduce the available power.

In flight applications, this is a system-level issue that requires evaluation to assess potential risks. This problem can potentially be compounded for systems that power-up at a reduced power dissipation state. In this situation, it may be desirable to add heaters, which serve both as startup and supplemental heaters, to the evaporator. To mitigate this problem, its important to minimize the effective thermal mass of the equipment attached to the evaporator. This is accomplished by providing thermal isolation between the equipment and the mounting interface and the surrounds.

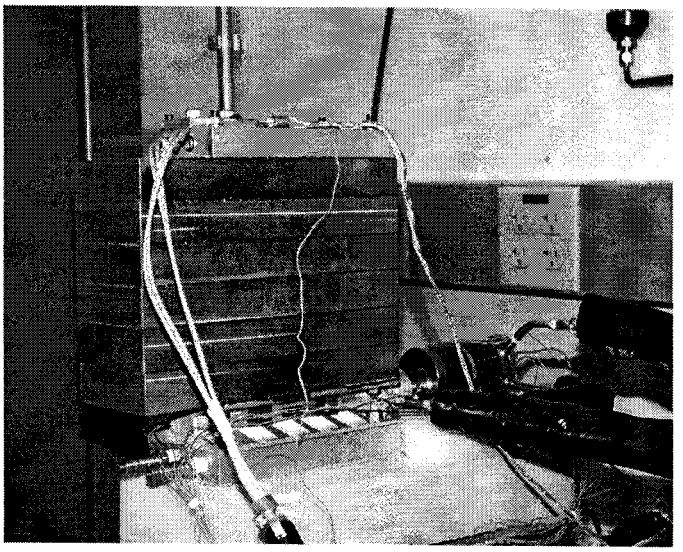

Figure 8. LHP evaporator with large mass: view of cooling block heat exchanger on bottom

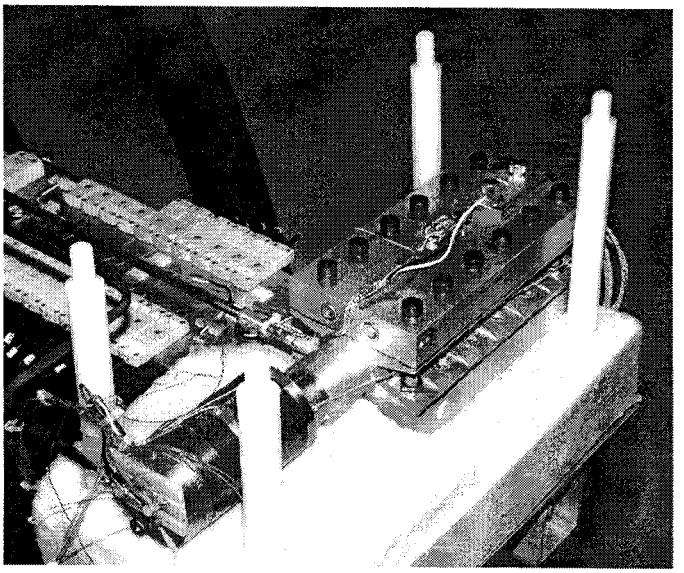

Figure 9. LHP evaporator with large mass: view of compensation chamber with heater and temperature sensor

A heater placed in the compensation chamber was implemented to study the temperature control capability of the LHP. A Minco Kapton thin film heater was bonded to the circumference of the compensation chamber and

silicon diode temperature sensor was bonded to the compensation chamber end-cap to control its temperature. The heater was sized for 15 W maximum dissipation. Fig. 9 shows the location of the heater and temperature sensor.

THEORETICAL BASIS FOR TEMPERATURE OSCILLATIONS

Investigations of temperature oscillations in two-phase thermal control systems are needed to understand the underlying mechanisms, which cause such behavior. These temperature oscillations effect the heat transfer characteristics of these systems and therefore, an increased understanding is needed to avoid potential problems in flight applications.

Previous experimental and numerical investigations have revealed temperature oscillations, which can be classified into three types:

(a) Low frequency temperature oscillations with amplitudes up to several tens of degrees Celsius and periods of oscillations up to several hours. This behavior leads to significant temperature variations for the evaporator and condenser.

(b) Medium frequency temperature oscillations having amplitudes in the order of several degrees Celsius. The oscillation periods are in the order of a few minutes up to tens of minutes. The maximum peak-to-peak variations are observed in the liquid line. The temperature variations observed for the evaporator and condenser are small.

(c) High frequency temperature oscillations which have been predicted to occur at the vapor-liquid interface in the evaporator wick structure.

From an engineering point of view, the first two types of temperature oscillations are of greater importance. In particular, the focus of this investigation is only on low frequency oscillations which have a greater effect on the heat transport characteristics of LHPs.

LHP behavior showing low frequency oscillations have been observed by a number of investigators [2,16]. Such behavior has also been demonstrated in numerical experiments using a mathematical model of a LHP [17]. Goncharov, et. al. [16] offers an explanation for initiation and termination of low frequency oscillations which is theoretically sound and is discussed in greater detailed in the next section.

The typical heat transport characteristics of LHPs is shown in Fig. 10. The temperature difference between the evaporator and condenser (ΔT_{e-c}) is plotted as a function of evaporator power input. Steady state results for the JPL LHP demonstration unit with ammonia and propylene are shown in Figs. 11 and 12, respectively. The characteristic behavior is evident with both working fluids. The performance curve shows that a LHP is able to operate at two different evaporator heat loads with the same temperature difference for $\Delta T_{e-c} > \Delta T_{min}$. The curve also shows a region where the LHP is not operable for conditions with $\Delta T_{e-c} < \Delta T_{min}$. It is also noted that when a large mass is attached to the evaporator, the actual evaporator heat load can vary significantly. When the evaporator and attached mass are cooled, the actual evaporator heat transfer to the condenser exceeds the applied evaporator heat load. Conversely, when the evaporator and mass are heated, the actual evaporator heat transfer to the condenser is less than the applied evaporator heat load. These conditions are valid when the attached mass has a significantly larger heat capacity than the evaporator. For transient conditions when the evaporator is being heated, the equation developed in the previous section applies:

$$Q_{LHP}=(m/(M+m))Q_{mass}$$

It is important to note that under steady state conditions, the heat capacity effects are not applicable.

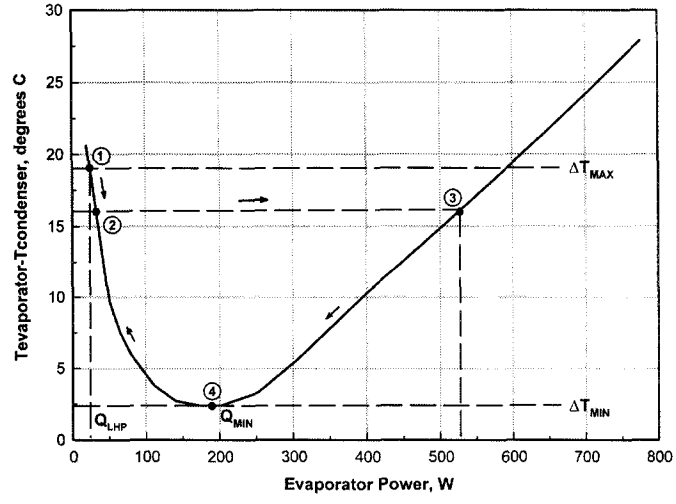

Figure 10. Typical heat transport characteristics of LHPs

During startup, if the actual evaporator heat load Q_{LHP} is less than Q_{min}, then LHP startup occurs at state point 1 in Fig. 10.

The operation proceeds to state point 2 as Q_{LHP} increases as a result of cooling the evaporator and mass. Operation can then move very quickly from state point 2 to 3. This occurs because when the highly subcooled liquid enters the compensation chamber, almost all the vapor is condensed. At this point, the LHP conductance increases significantly. Transition from state point 2 to 3 occurs only if the thermal inertia effects increase the evaporator heat transfer to values greater than Q_{min}. The operation continues along state point 3 to

4 where the LHP has a fairly constant conductance. Consequently, the temperature difference (ΔT_{e-c}) decreases to ΔT_{min} and the evaporator heat load (Q_{LHP}) decreases to Q_{min}. As the evaporator heat load decreases further, the evaporator temperature begins to rise. The entire cycle with state points 1-2-3-4 can then be repeated leading to stable temperature oscillations. Conditions leading to stable temperature oscillations depend on the external environment, the attached mass heat capacity and the difference between Q_{LHP} and Q_{min}. Stable low frequency temperature oscillations were predicted using a LHP mathematical model developed by Sasin et. al., [17]. The predicted oscillations are shown in Fig. 13. The results shown are for a propylene LHP with a 5 W applied evaporator heat load. The temperature amplitude is about 50°C peak-to-peak with an oscillation period of about 5 hours.

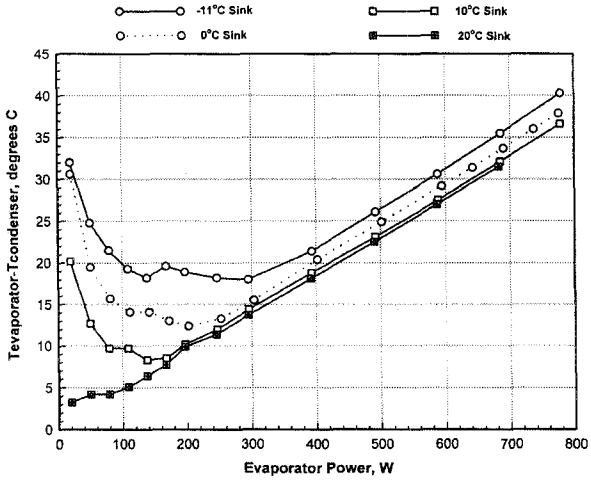

Figure 11. Steady state results with ammonia working fluid: JPL LHP demonstration unit without attached large mass [1]

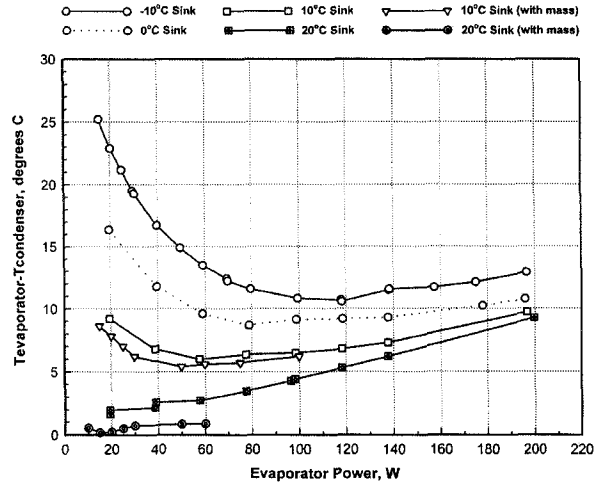

Figure 12. Steady state results with propylene working fluid: JPL LHP demonstration unit without large attached mass

TEST PROGRAM

Thermal testing was carried out at various temperature conditions for the condenser and evaporator as well as power levels. Evaporator power and sink temperature was varied from 15 to 75 W and –30 to 0°C, respectively. These tests are a subset of the complete characterization tests performed on this unit.

This paper reports only on test results, which show low frequency transient temperature oscillations. These tests were only performed for the horizontal position where condenser and evaporator are approximately at the same elevation and with the large mass attached to the evaporator. This was done to simulate on-orbit microgravity conditions for the TES LHPs.

SUMMARY OF TEST RESULTS

Results showing stable low frequency temperature oscillations are shown in Figs. 14-27. The evaporator and compensation chamber temperatures plotted are average values from four and six thermocouples, respectively. Table 2 correlates temperature labels used in the plots with the thermocouple locations from Fig. 6. Qevap is the power applied to the heater block at the evaporator.

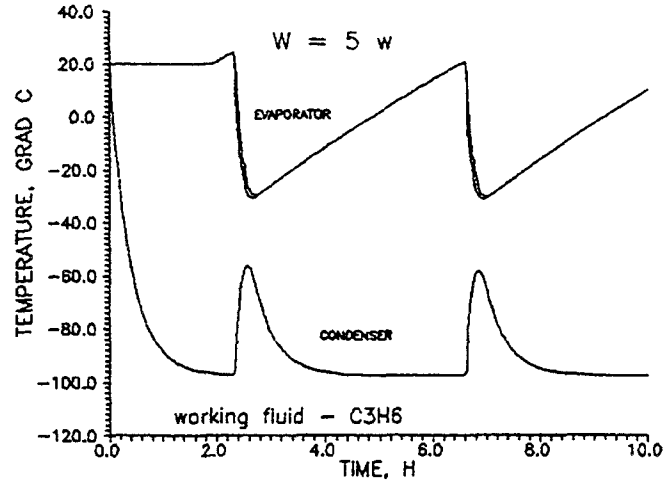

Figure 13. Predicted temperature oscillations using mathematical model [17]

Figs. 14-18 show the development of stable oscillations from startup with a constant sink temperature and evaporator power. Figs. 19-22 show results when the sink temperature is changed while the evaporator power remains constant. Results for conditions when the sink temperature is fixed and the evaporator power is changed in a step-wise mode are shown in Figs. 23-27. The results show that these oscillations are stable and repeatable. The oscillatory behavior is repeatable in that if the evaporator power or sink temperature are changed to produce stable operation without oscillations and then

conditions are returned to the original settings, the same oscillatory behavior is produced.

Table 2. Definition of temperature labels

Plot Label	Thermocouple No.
Tevap	TC1 – TC4 Average
Tcc	TC7 – TC12 Average
Tliq-exit	TC22
Tliq	TC40
Tvap-in	TC21
Trad	TC27, TC33, TC38 Average
Tvap	TC24
Tamb	TC20

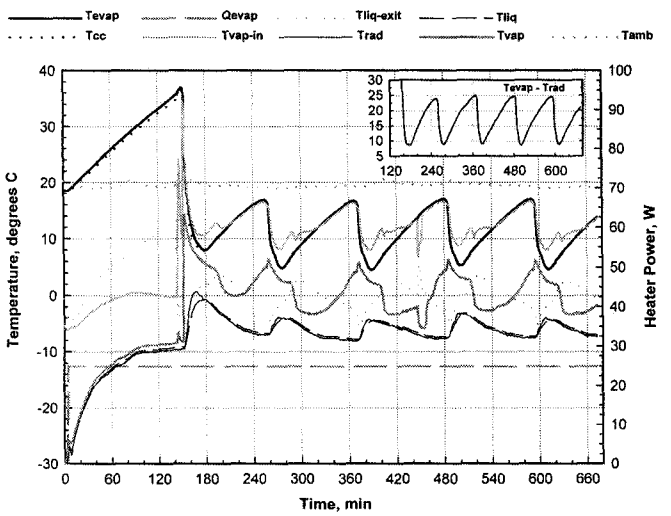

Figure 14. Results for 25W to evaporator and –10°C sink temperature

The temperature amplitude as a function of evaporator power and sink temperature for all test cases is shown in Fig. 28. The results show that as the evaporator power increases, the temperature amplitude decreases almost linearly. The temperature amplitude increases as the sink temperature is reduced. The oscillation period as a function of evaporator power and sink temperature is plotted in Fig. 29 for all test cases. Again as the evaporator power increases the oscillation period decreases. The oscillation period is higher for lower sink temperatures.

Temperature amplitudes in the tens of degrees Celsius with oscillation periods of up to several hours have been observed in the operation of a propylene LHP with a large mass attached to the evaporator. These low frequency oscillations have been observed for sink temperatures as high as 0°C. Testing done with sink temperatures above 0°C showed no signs of these low frequency oscillations. These oscillations were also observed for evaporator power level of up to 75 W with a sink of –15°C.

The maximum heat transfer to the condenser while cooling the large mass was estimated by determining the sensible heat loss as a function of time. The results are plotted in Fig. 30 and clearly show that these heat transfer rates correspond to the constant conductance region from Fig. 12.

The theory proposed by Goncharov, et. at., [16] to explain this phenomena is consistent with the results reported in this work. The nature of the low frequency oscillations reported by Gorcharov's team is similar to the observations made in these tests.

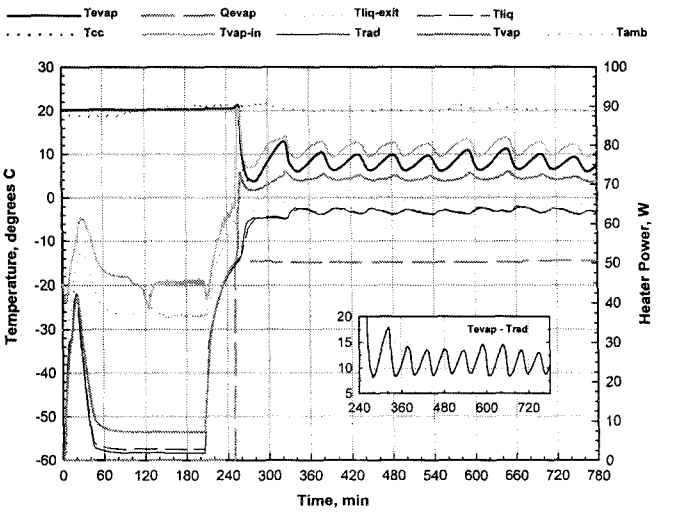

Figure 15. Results for 50 W to evaporator and –10°C sink temperature

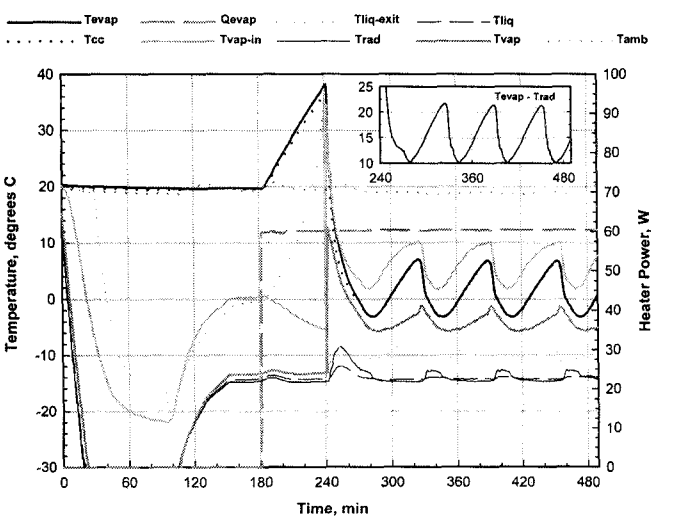

Figure 16. Results for 60 W to evaporator and –15°C sink temperature

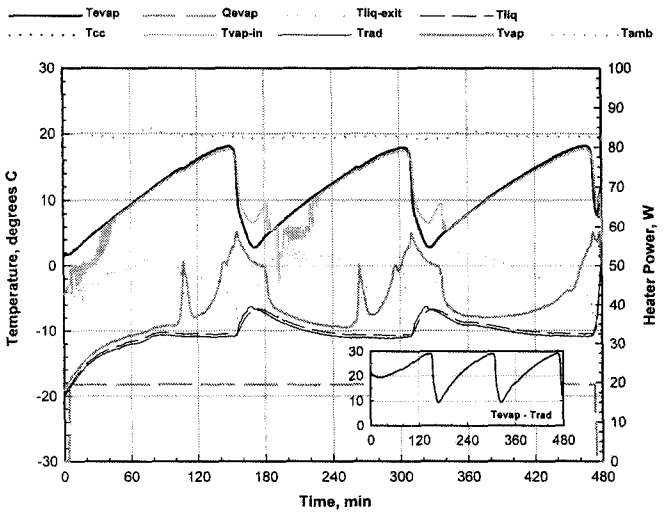

Figure 17. Results for 20 W to evaporator and –10°C sink temperature

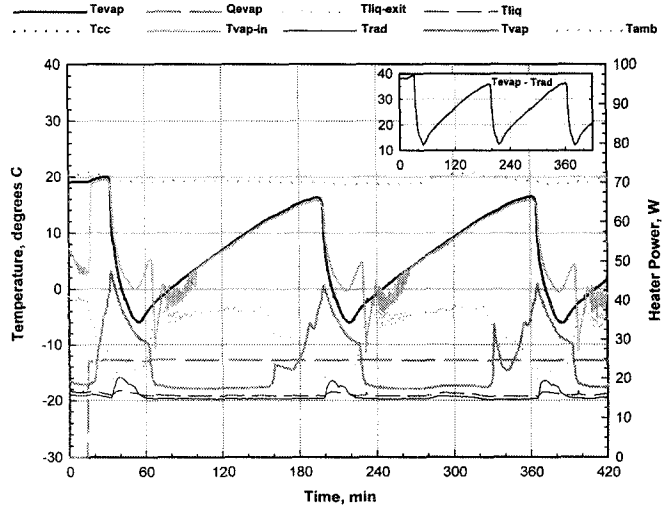

Figure 18. Results for 25 to evaporator and –20°C sink temperature

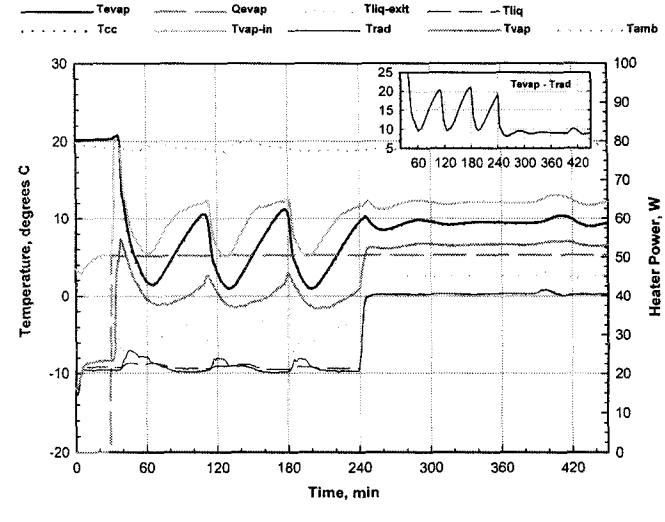

Figure 19. Results for 50 W to evaporator and –10°C and 0°C sink temperatures

Test results have demonstrated large amplitude temperature oscillations at low power levels and temperatures below ambient levels. The temperature amplitudes and oscillation periods are stable and repeatable. Once startup occurred the oscillations were predictable and stable. The initial conditions prior to startup appeared not to effect the nature of the oscillations.

CONCLUSION

Characterization testing has been performed on a propylene LHP technology demonstration unit of similar design to the flight units for the TES instrument. Evaluation of the test results presented in this paper revealed low frequency temperature oscillation phenomena. The observations are consistent with the results of previous investigators both experimental and numerical.

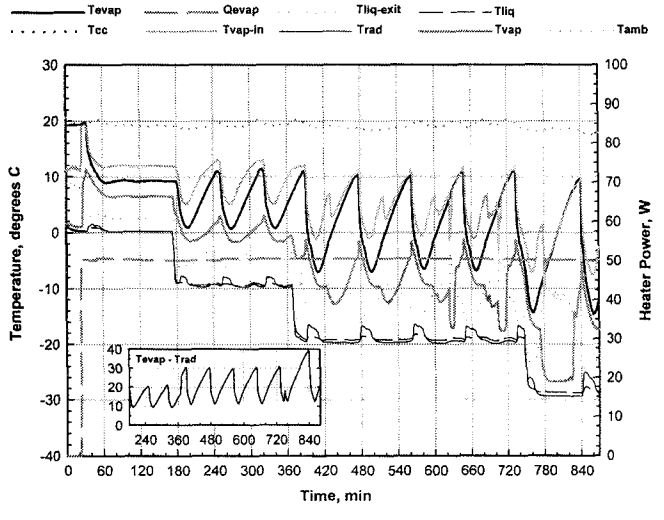

Figure 20. Results for 50W to evaporator and –10°C, -20°C and –30°C sink temperatures

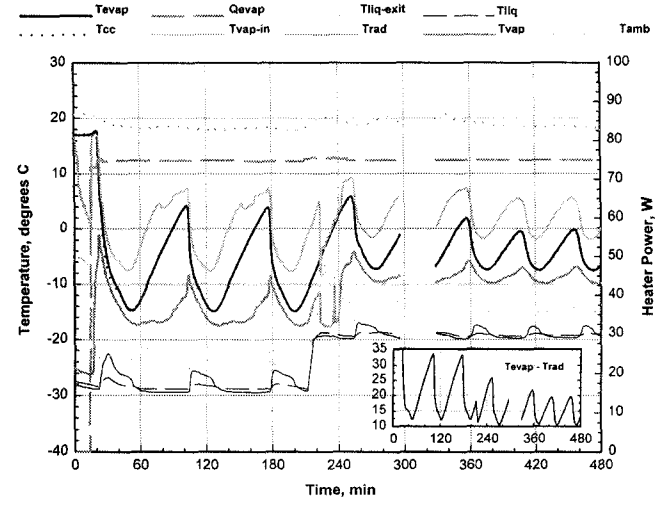

Figure 21. Results for 75 W to evaporator and –30°C and –20°C sink temperature

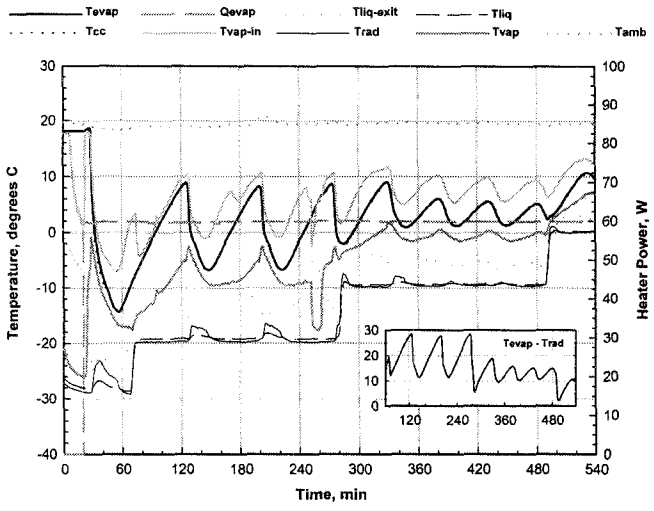

Figure 22. Results for 60 W to evaporator and –20°C, -10°C and 0°C sink temperature

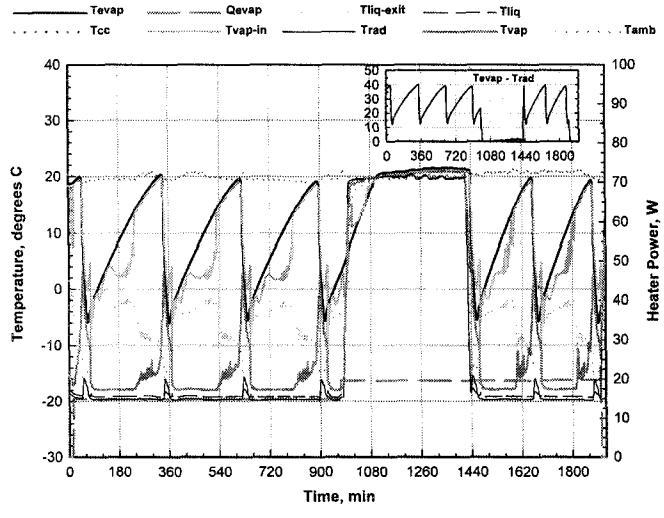

Figure 23. Results for 15 W and 20 W to evaporator and –20°C and 20°C sink temperatures

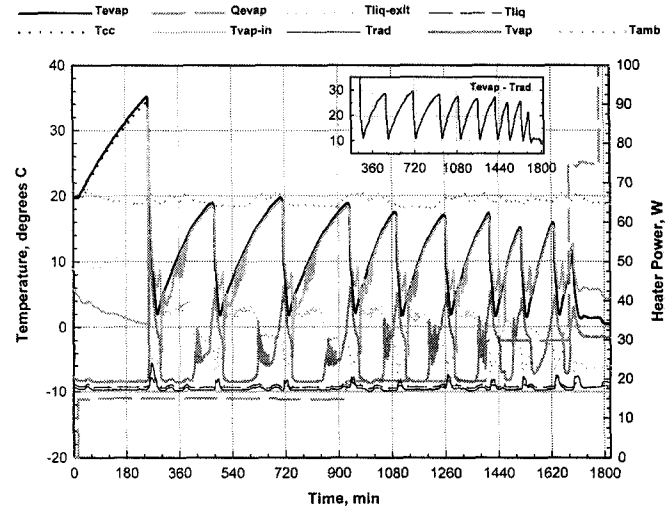

Figure 24. Results for 15 W, 20 W and 30 W to evaporator and –10°C sink temperature

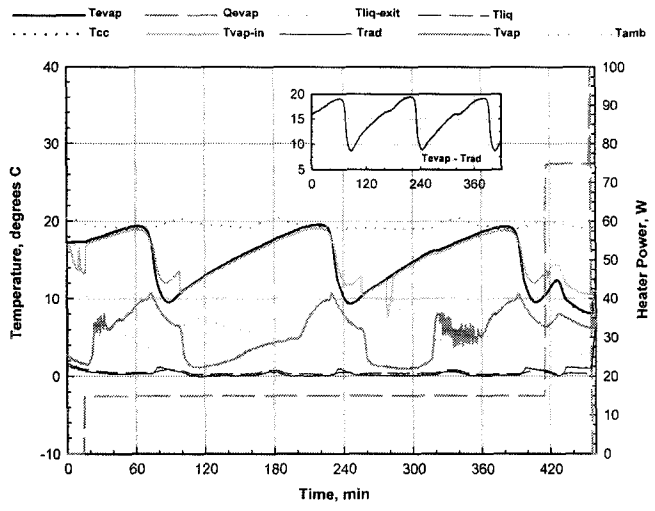

Figure 25. Results for 15 W and 75 W to evaporator and 0°C sink temperature

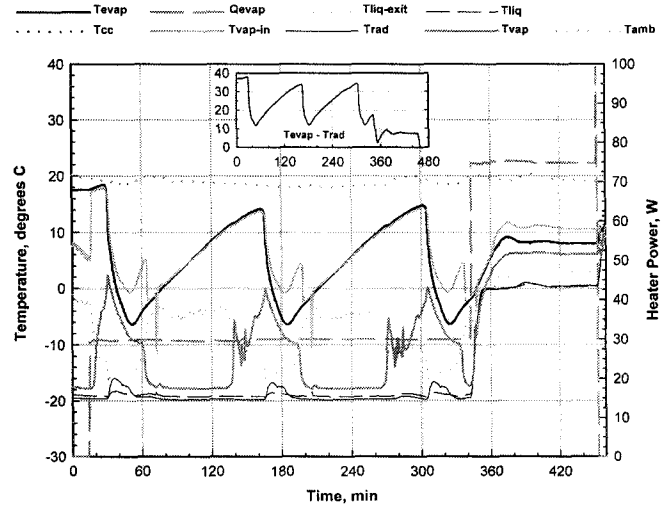

Figure 26. Results for 30 W and 75 W to evaporator and –20°C sink temperature

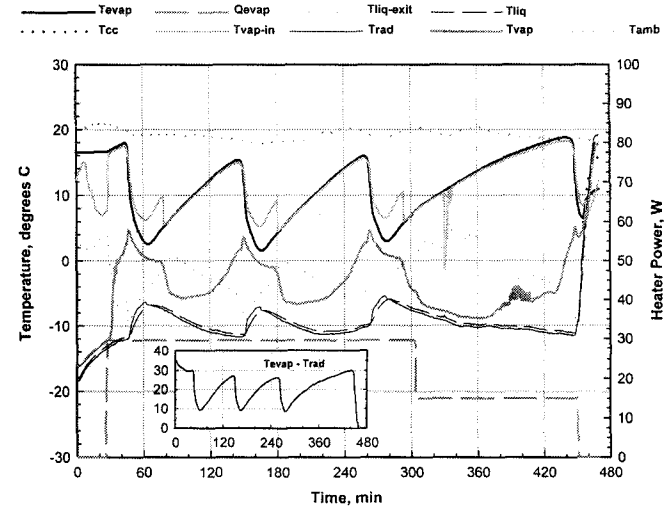

Figure 27. Results for 30 W and 15 W to evaporator and –10°C sink temperature

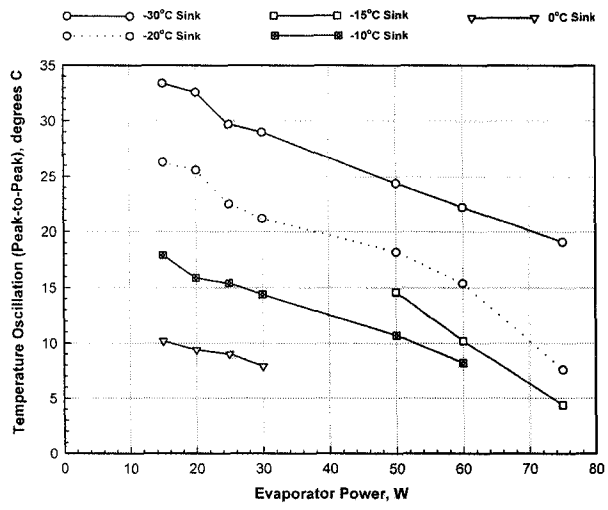

Figure 28. Transient temperature amplitudes with low frequency oscillations

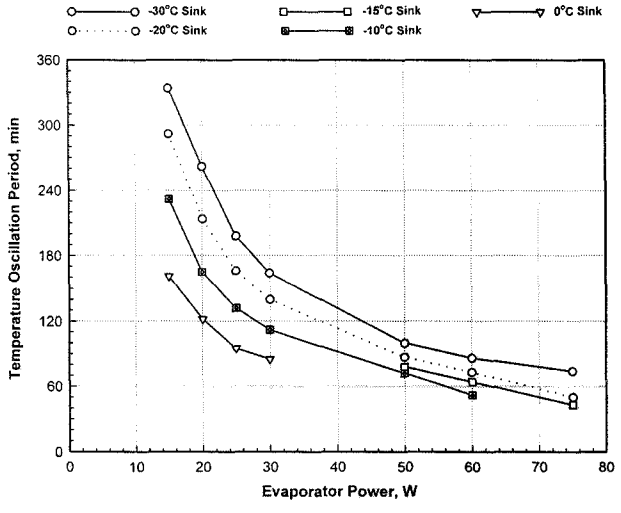

Figure 29. Temperature oscillation period for low frequency oscillations

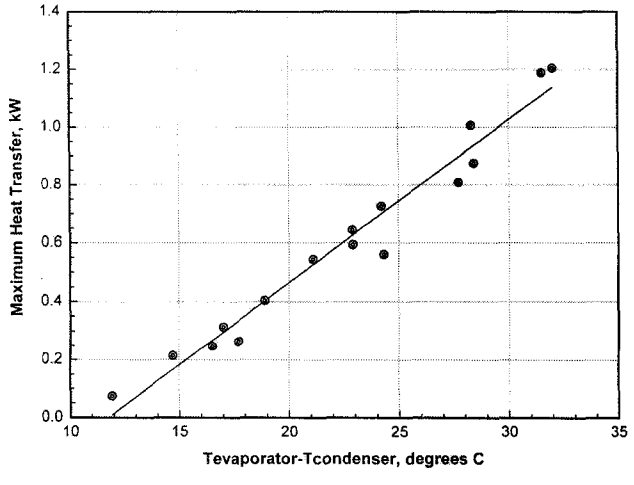

Figure 30. Maximum heat transfer to condenser when large mass is being cooled

Low frequency temperature oscillation phenomena was observed for conditions with low power and sink temperatures as high as 0°C. These phenomena resulted in excessive temperature extremes. Under some conditions, temperature amplitudes up to 34°C and periods of oscillation up to 5.5 hours were observed. In general, lower power and sink temperatures produced higher amplitudes with increasing periods of oscillation. This phenomena is not affected by initial startup conditions and it is very stable and repeatable.

Results from this investigation has revealed that this phenomena is predictable and must be taken into account when designing systems with LHPs for space applications. This oscillatory behavior can have a very significant impact on space systems, particularly when temperature stability affects performance. Additional testing is required to fully understand the dynamics of these low frequency oscillations. In particular, testing in vacuum conditions is needed to understand the effects of parasitic heat leaks. In addition, transient mathematical models are needed with hydrodynamic and transport processes model appropriately to predict this phenomena reliably. It is recommended that transient testing be done in conjunction with the numerical simulations to validate the models.

ACKNOWLEDGMENTS

The authors would like to thank Scott Leland and Jose Rivera for helping to setup the JPL LHP test bed. Special thanks to Michael Nikitkin, Dave Feenan and Bill Kroutiack from Dynatherm Corporation Inc. in Hunt Valley, Baltimore who supplied the LHP demonstration unit and provided valuable inputs. We would like to recognize the support of the TES project manager Tom Glavich, the TES team as well as our supervisor Dr. Ron Ross.

The research described in this paper was carried out at the Jet Propulsion Laboratory, California Institute of Technology, under a contract with the National Aeronautics and Space Administration.

REFERENCES

1. Pauken, M. and Rodriguez, J.I., "Performance Characterization and Model Verification of a Loop Heat Pipe," 30th SAE Technical Paper Series, Paper No. 2000-01-2317, Toulouse, France, July 2000.
2. Rodriguez, J.I., "Transient Characterization of a Propylene Loop Heat Pipe During Startup and Shut-Down," 30th SAE Technical Paper Series, Paper No. 2000-01-2408, Toulouse, France, July 2000.
3. Goncharov, K.A., Nikitkin, M.N., Golovin, O.A., Fershtater, Y.G., Maidanik, Y.F. and Piukov, S.A., "Loop Heat Pipes in Thermal Control Systems for OBZOR Spacecraft," 25th ICES, SAE Technical Paper Series, Paper No. 951555, July 1995.
4. Orlov, A.A., Goncharov, K.A., Kotlyarov, E.Y. and Tyklina, T.A., "The Loop Heat Pipe Experiment on Board the

GRANAT Spacecraft," 6th European Symposium on Space Environmental and Control Systems, Noordwijk, Netherlands, 1997.
5. Ku, J., "Operating Characteristics of Loop Heat Pipes," SAE Paper No. 1999-01-2007, July 1999.
6. Nikitkin, M., and Cullimore, B., "CPL and LHP Technologies: What are the Differences, What are the Similarities?," SAE Technical Paper Series, Paper No. 981587, July 1998.
7. Maidanik, Y.F., Fershtater, Y.G. and Solodovnik, N.N., "Loop Heat Pipes: Design, Investigation, Prospects of Use in Aerospace Technics," SAE Technical Paper Series, Paper No. 941185, April 1994.
8. Wolf, D.A., Ernst, D.M. and Phillips, A.L., "Loop Heat Pipes – Their Performance and Potential," SAE Technical Paper Series, Paper No. 941575, June 1994.
9. Maidanik, Y.F., et al., "Development and Experimental Investigation of Loop Heat Pipes," 7th International Heat Pipe Conference, 1990.
10. Maidanik, Y.F., Fershtater, Y.G., Pastukhov, V.G., Vershinin, S.V. and Goncharov, K.A., "Some Results of Loop Heat Pipes Development, Tests and Application in Engineering," 5th International Heat Transfer Symposium, Melbourne, Vic., 1996.
11. Maidanik, Y., Vershinin, S., Solodovnik, N., Gluck, D., and Gerhart, C., "Some Results of the Latest Developments and Tests of Loop Heat Pipes," 33rd Intersociety Energy Conversion Conference, LaGrange Park, IL, 1998.
12. Kaya, T., Hoang, T.T., Ku, J. and Cheung, M.K., "Mathematical Modeling of Loop Heat Pipes," 37th Aerospace Science Meeting and Exhibit, Paper No. AIAA 99-0477, January 1999.
13. Cheung, M.K., Hoang, T.T., Ku, J. and Kaya, T., "Thermal Performance and Operational Characteristics of Loop Heat Pipes (NRL LHP)," SAE Technical Paper Series, Paper No. 981813, July 1998.
14. Douglas, D., Ku., J. and Kaya, T., "Testing of the Geoscience Laser Altimeter System Prototype Loop Heat Pipe," 37th Aerospace Science Meeting and Exhibit, Paper No. AIAA 99-0473, January 1999.
15. Rodriguez, J.I., "Thermal Design of the Tropospheric Emission Spectrometer Instrument," 30th SAE Technical Paper Series, Paper No. 2000-01-2274, Toulouse, France, July 2000.
16. Goncharov, K.A., Kotlyarov, E. Yu., Smirnov, F. Yu., Schlitt, R., Beckmann, K., Meyer, R. and Muller, R., "Investigation of Temperature Fluctuations in Loop Heat Pipes," 24th SAE Technical Paper Series, Paper No. 941577, Friedrichshafen, Germany, June 1994.
17. Sasin, V.Y., Zelenov, I.A., Zuev, V.G and Kotlyarov, E.Y., "Mathematical Model of a Capillary Loop Heat Pipe with a Condenser-Radiator," 20th SAE Technical Paper Series, Paper No. 901276, Williamsburg, Virginia, July 1990.

CONTACT

For additional information contact: Dr. Jose I. Rodriguez at the Jet Propulsion Laboratory. Phone:(818)354-0799. Email: Jose.I.Rodriguez@jpl.nasa.gov